Hsp70 and Hsp40 Chaperones Do Not Modulate Retinal Phenotype in SCA7 Mice

Dominique Helmlinger, Jacques Bonnet, Jean-Louis Mandel, Yvon Trottier, Didier Devys

THE JOURNAL OF BIOLOGICAL CHEMISTRY
Vol. 279, No. 53, Issue of December 31, pp. 55969–55977, 2004

Printed in U.S.A.

Hsp70 and Hsp40 Chaperones Do Not Modulate Retinal Phenotype in SCA7 Mice*♦

Received for publication, August 9, 2004, and in revised form, September 17, 2004
Published, JBC Papers in Press, October 19, 2004, DOI 10.1074/jbc.M409062200

Dominique Helmlinger‡§, Jacques Bonnet‡, Jean-Louis Mandel‡, Yvon Trottier‡, and Didier Devys‡¶

From the ‡Department of Molecular Pathology, Institut de Génétique et de Biologie Moléculaire et Cellulaire, CNRS/INSERM/ULP/Collège de France, BP 10142, 67404 Illkirch Cedex, France

Nine neurodegenerative diseases, including spinocerebellar ataxia type 7 (SCA7), are caused by the expansion of polyglutamine stretches in the respective disease-causing proteins. A hallmark of these diseases is the aggregation of expanded polyglutamine-containing proteins in nuclear inclusions that also accumulate molecular chaperones and components of the ubiquitin-proteasome system. Manipulation of HSP70 and HSP40 chaperone levels has been shown to suppress aggregates in cellular models, prevent neuronal death in *Drosophila*, and improve to some extent neurological symptoms in mouse models. An important issue in mammals is the relative expression levels of toxic and putative rescuing proteins. Furthermore, overexpression of both HSP70 and its co-factor HSP40/HDJ2 has never been investigated in mice. We decided to address this question in a SCA7 transgenic mouse model that progressively develops retinopathy, similar to SCA7 patients. To co-express HSP70 and HDJ2 with the polyglutamine protein, in the same cell type, at comparable levels and with the same time course, we generated transgenic mice that express the heat shock proteins specifically in rod photoreceptors. While co-expression of HSP70 with its co-factor HDJ2 efficiently suppressed mutant ataxin-7 aggregation in transfected cells, they did not prevent either neuronal toxicity or aggregate formation in SCA7 mice. Furthermore, nuclear inclusions in SCA7 mice were composed of a cleaved mutant ataxin-7 fragment, whereas they contained the full-length protein in transfected cells. We propose that differences in the aggregation process might account for the different effects of chaperone overexpression in cellular and animal models of polyglutamine diseases.

Spinocerebellar ataxia type 7 (SCA7)[1] is a dominantly inherited neurodegenerative disorder, characterized by late-onset neuronal loss in cerebellum, brainstem, and retina (1). SCA7 is caused by an abnormal expansion of a polyglutamine (poly(Q)) tract (38–460 repeats) in the SCA7 gene product ataxin-7 (2), a 892-amino acid protein recently identified as a new component of a multisubunit transcriptional complex (3). Eight other neurodegenerative diseases are caused by a CAG/poly(Q) repeat expansion, including Huntington disease (HD), dentatorubro-pallidoluysian atrophy, spinobulbar muscular atrophy (SBMA) and spinocerebellar ataxia types 1, 2, 3, 6, and 17. Genetic and molecular studies indicate that poly(Q) tracts confer a novel toxic function to the otherwise unrelated proteins, but the mechanisms by which poly(Q) expansions lead to neurodegeneration remain unclear (4, 5).

All of these diseases are characterized by continuous accumulation of mutant proteins in insoluble aggregates, typically forming nuclear inclusions (NIs) (6). NIs have been shown to stain positively for ubiquitin, chaperones (mainly heat shock proteins), and proteasome subunits, in various cellular and animal models of poly(Q) diseases, as well as in post-mortem patient brains (7, 8). Several SCA7 mouse models, which reproduce many features of the human situation, display numerous NIs consistently stained for ubiquitin, proteasome subunits, and chaperones (HSP70, HSC70, and HDJ2) (9–12). In SCA7 patient brains, HDJ2, ubiquitin, and 19 S proteasome subunits co-localize with NIs (13–15). Furthermore, the levels of several chaperones, including the HSP70 and the HSP40 chaperones HDJ1 and HDJ2, were shown to be reduced in SCA7 and/or HD mouse models (16, 17). Altogether, these findings suggested that protein misfolding and impaired clearance might be a common pathogenic event in poly(Q) diseases. Accordingly, several studies showed that overexpression of chaperones in cells reduces aggregate formation and, in some cases, suppresses poly(Q) toxicity (reviewed in Refs. 8 and 18). Genetic screens, in *Drosophila* models overexpressing mutant ataxin-1 or a pure 127Q stretch, identified molecular chaperones and components of the ubiquitin-proteasome pathway as strong modulators of poly(Q)-induced toxicity (19, 20). In particular, deletion of HSP70 genes exacerbated SCA1 or SBMA fly phenotypes, whereas overexpression of HSP70 or HDJ1 suppressed neurodegeneration in various *Drosophila* models (19–24). Furthermore, Chan *et al.* (25) showed that HSP70 and HDJ1 synergistically suppressed poly(Q) toxicity in a SCA3 fly model. These chaperones work together in an ATP-dependent manner, notably to help refold denaturated and aggregated proteins. HSP40 co-chaperones recognize abnormally folded polypeptide substrates, present them to HSP70, and stimulate HSP70 ATPase activity (26).

* This work was supported by grants from the Hereditary Disease Foundation and from the European Community (EUROSCA integrated Project LSHM-CT-2004-503304), funds from the Institut National de la Santé et de la Recherche Médicale, the Centre National de la Recherche Scientifique, and the Hôpital Universitaire de Strasbourg (HUS). The costs of publication of this article were defrayed in part by the payment of page charges. This article must therefore be hereby marked "*advertisement*" in accordance with 18 U.S.C. Section 1734 solely to indicate this fact.

♦ This article was selected as a Paper of the Week.

§ Supported by a fellowship from the Fondation pour la Recherche Médicale.

¶ To whom correspondence should be addressed. Tel.: 33-388-65-34-13; Fax: 33-388-65-32-46; E-mail: devys@igbmc.u-strasbg.fr.

[1] The abbreviations used are: SCA7, spinocerebellar ataxia type 7; poly(Q), polyglutamine; HD, Huntington disease; SBMA, spinobulbar muscular atrophy; NI, nuclear inclusion; HSP (or Hsp), heat shock protein; ERG, electroretinogram; HA, hemagglutinin; DAPI, 4,6-diaminido-2-phenylindole; RT, reverse transcription; WT, wild-type.

Overexpression of HSP70 had a more mitigated outcome in modulating poly(Q) toxicity in mouse models (17, 27, 28). The authors hypothesized that this might be explained by the lack of HSP40 induction that would be required for HSP70 to modulate neurodegeneration. Overexpression of both HSP70 and HSP40 has not been investigated in mouse models of poly(Q) diseases. We decided to address this question in a SCA7 transgenic mouse model that presents with a progressive and severe retinopathy (9, 29). In this model, neuronal dysfunction of a single cell type (rod photoreceptors) can be quantified on living animals by recording electroretinograms (ERGs). To co-express mutant ataxin-7 and the molecular chaperones in the same cell type, we generated transgenic mice overexpressing HSP70 and HDJ2 specifically in rod photoreceptors. These heat shock proteins efficiently suppressed mutant ataxin-7 aggregation in transfected cells but were not able to prevent either neuronal toxicity or aggregate formation in photoreceptors from SCA7 mice. We show here for the first time that expressing both HSP70 and its co-factor HDJ2 has no beneficial effect on phenotype progression in a poly(Q) mouse model.

EXPERIMENTAL PROCEDURES

Generation of Transgenic Animals—A 2.2-kb XbaI-SmaI fragment of the human rhodopsin promoter, encompassing the distal enhancer region, was subcloned from the R7N construct (9) into the pGSp2 vector, kindly provided by Dr. D. Metzger, upstream of the rabbit β-globin intron II, to generate the pGS-Rho vector. The 1.9-kb human HSP70 cDNA was amplified by PCR from clone pH2.3, kindly provided by Dr. R. Morimoto, using a 5′ primer encoding a FLAG epitope. The 1.2-kb human HDJ2 cDNA was amplified by PCR from clone J3, kindly provided by Dr. T. Mohanakumar, using a 3′ primer encoding a HA epitope. These PCR fragments were XhoI-NheI-digested and cloned into the pGS-Rho vector to generate pGS-Rho-RH70 and pGS-Rho-RH40 transgene constructs, respectively. All final plasmids were verified by sequencing and subsequently SalI-ApaLI-digested to remove bacterial sequences, purified on sucrose gradients, and microinjected into FVB/N-fertilized eggs, as described (9). Mouse tail DNA was screened by PCR for the presence of the transgenes. Founder mice were backcrossed on the inbred C57BL/6 background to get F3 RH40 or RH70 transgenic mice with a mixed (87.5% C57BL/6; 12.5% FVB/N) genetic background. The loss of the *rd* allele from the FVB/N background was checked by PCR followed by DpnI digestion. For genotyping of R7E, RH70, and RH40 transgenic mice, mouse tail DNA was screened by PCR using specific primers (5′-AGGCGATGACAAAGAAGAG-3′ and 5′-AGGGGATGAGGATGAAGAG-3′ for the *SCA7* transgene, 470-bp product; 5′-CAACAAGATCACCATCACCAAC-3′ and 5′-GCTATTGCTTTATTTGTAACC-3′ for the *HSP70* transgene, 500-bp product; 5′-GGGGTCAAACCCAATGCTACTC-3′ and 5′-CATCCTTCCTCCTCCTCCAAAA-3′ for the *HDJ2* transgene, 260-bp product). For genotyping of double and triple transgenic mice, two independent PCR reactions were performed on the same mouse tail DNA sample; one including both *HSP70* and *HDJ2* primer pairs and another using primers specific for the *SCA7* transgene.

Plasmid Construction and Cell Transfection—For cell transfection experiments, a full-length *SCA7* cDNA with 128 CAGs was obtained by PCR amplification of the B7E2B construct (10), using a 5′ primer encoding a FLAG epitope. This fragment was subcloned into pcDNA3.1(+) (Invitrogen) to generate pc7E2FL. A truncated *SCA7* construct (pc7E2–456) was generated by PCR amplification of pc7E2FL and introduced into pcDNA3.1(+) vector (Invitrogen). Tagged full-length *HDJ2* and *HSP70* cDNAs were subcloned from pGS-Rho-RH70 and pGS-Rho-RH40 constructs into pcDNA3.1(+) (Invitrogen) to generate pcHDJ2 and pcHSP70 constructs, respectively. 2×10^5 HEK293T cells were transiently transfected by calcium phosphate precipitation, washed 16 h later, and harvested or fixed 24 or 48 h after washing.

Immunoblot Blot Analysis—Whole cell extracts from dissected retina or from transfected HEK293T cells were obtained by homogenization in lysis buffer containing 50 mM Tris-HCl, pH 8.0, 10% glycerol, 5 mM EDTA, 150 mM KCl, 0.5% Nonidet P-40, 1 mM phenylmethylsulfonyl fluoride, and a mixture of protease inhibitors. Homogenates were then incubated for 20 min on ice and centrifuged for 30 min at 10,000 × *g* and 4 °C. Supernatants were resolved on 8% SDS-PAGE gels. Primary antibodies used were mouse monoclonal anti-FLAG M2 (Sigma), anti-HA 12CA5, anti-HSP70 SPA-810 (Stressgen, Victoria, Canada), and anti-HDJ2/Hsp40 (Neomarkers, Fremont, CA).

Antibody Production—The anti-ataxin-7 polyclonal 1599 antibody was generated by immunization of rabbits with a peptide corresponding to amino acids 226–245 (KEKLQLRGNTRPMHPIQQSR) of human ataxin-7 and purified as described previously (9).

Immunohistology and Light Microscopy—For histology, retina were dissected from enucleated eyes and then fixed by immersion in 2.5% glutaraldehyde. Fixed eyes were rinsed in phosphate-buffered saline, dehydrated with a graded alcohol series, and embedded in Epon. Semithin (1 μm) sections were stained with toluidin blue. For immunocytofluorescence, transfected HEK293T cells were fixed in 4% paraformaldehyde and stained with anti-ataxin-7 2A10 monoclonal and affinity-purified 1261 and 1598 polyclonal antibodies, as described (9, 10). Immunohistofluorescence staining was performed as described previously (29). Briefly, dissected retina were fixed in 4% paraformaldehyde, cryoprotected, and frozen in Cryomatrix (Thermo Shandon). 10-μm cryostat sections were permeabilized, blocked, and then immunostained using the following primary antibodies: anti-ataxin-7 2A10 monoclonal and affinity-purified 1261, 1599, and 1598 polyclonal antibodies, as described (9, 10), anti-FLAG M2 (Sigma), anti-HA 12CA5, anti-HSP70 SPA-810 (Stressgen), and anti-HDJ2/Hsp40 (Neomarkers, Fremont, CA) mouse monoclonal antibodies. Secondary antibodies used were CY3- and Oregon Green-conjugated goat anti-rabbit and anti-mouse IgG (Jackson ImmunoResearch, West Grove, PA). Nuclei were counterstained with 0.5 μg/ml 4,6-diaminido-2-phenylindole (DAPI).

Real-time RT-PCR Analysis of Retinal RNA—Real-time RT-PCR analysis was performed as described previously (29). Briefly, reverse-transcribed total retinal RNA was amplified with SYBR Green I (Sigma) on a Light-Cycler instrument (Roche Applied Science, Basel, Switzerland) using *Rho*- and *Ppia*-specific primers.

Electroretinogram Recordings—Electroretinographic analysis was performed as described previously (29). Briefly, dark-adapted mice were anesthetized, pupils were dilated, and the cornea was locally anesthetized. Scotopic rod ERGs were recorded by using a gold loop electrode placed on the corneal surface and calibrated to a reference electrode inserted subcutaneously on the head. Light stimulation was increased from −4 to 1.4 log candela s m^{-2}, as measured with a luxmeter at eye level. The duration of the light stimulus was constant. Responses were digitized using a data acquisition labmaster board (Multiliner Vision).

RESULTS

Molecular Chaperones Suppress Formation of Aggregates in Cells Expressing Mutant Ataxin-7—We first evaluated whether overexpression of HSP70 and/or HSP40/HDJ2 could modulate mutant ataxin-7 aggregation in mammalian cells. We transfected HEK293T cells with truncated or full-length mutant *SCA7* cDNA constructs (128 CAG) either alone or together with human *HSP70*- and *HDJ2*-tagged cDNA constructs. Fourty hours after transfection, Western blots revealed high and comparable expression of FLAG-tagged mutant ataxin-7, FLAG-tagged HSP70, and HA-tagged HDJ2 (Fig. 1*A*). We then performed immunofluorescence staining of transfected cells using an N-terminal anti-ataxin-7 antibody (1261 (9)). While truncated (residues 1–456) and full-length normal ataxin-7 displayed a diffuse nuclear staining (3), mutant ataxin-7 either showed a similar localization or accumulated into large NIs (Fig. 1*B*, *upper panels*). Co-transfection of both *HDJ2* and *HSP70* cDNAs with truncated (residues 1–456) or full-length mutant *SCA7* completely suppressed formation of NIs (Fig. 1*B*, *lower panels* and data not shown). All transfected cells displayed a diffuse nuclear staining suggesting that overexpression of these chaperones inhibited mutant ataxin-7 aggregation. We then quantified this effect by counting cells displaying either NIs or homogenous nuclear staining after transfecting either truncated mutant *SCA7* cDNA alone or together with *HDJ2*, with *HSP70*, or with both *HDJ2* and *HSP70* cDNAs. Overexpression of HDJ2 had a mild effect on the number of aggregates (20.3% ± 2.6% *versus* 31.3% ± 2.7%) that was not statistically significant (one-way analysis of variance, $F_{(2,14)} = 1.6$, $p > 0.05$). Drastic suppression of aggregate formation was achieved by overexpressing HSP70 alone (1.0% ± 0.5% *versus* 31.3% ± 2.7%; one-way analysis of variance, $F_{(3,14)} = 4.8$, $p < 0.05$), or together with its co-factor HDJ2 (Fig. 1*C*). These

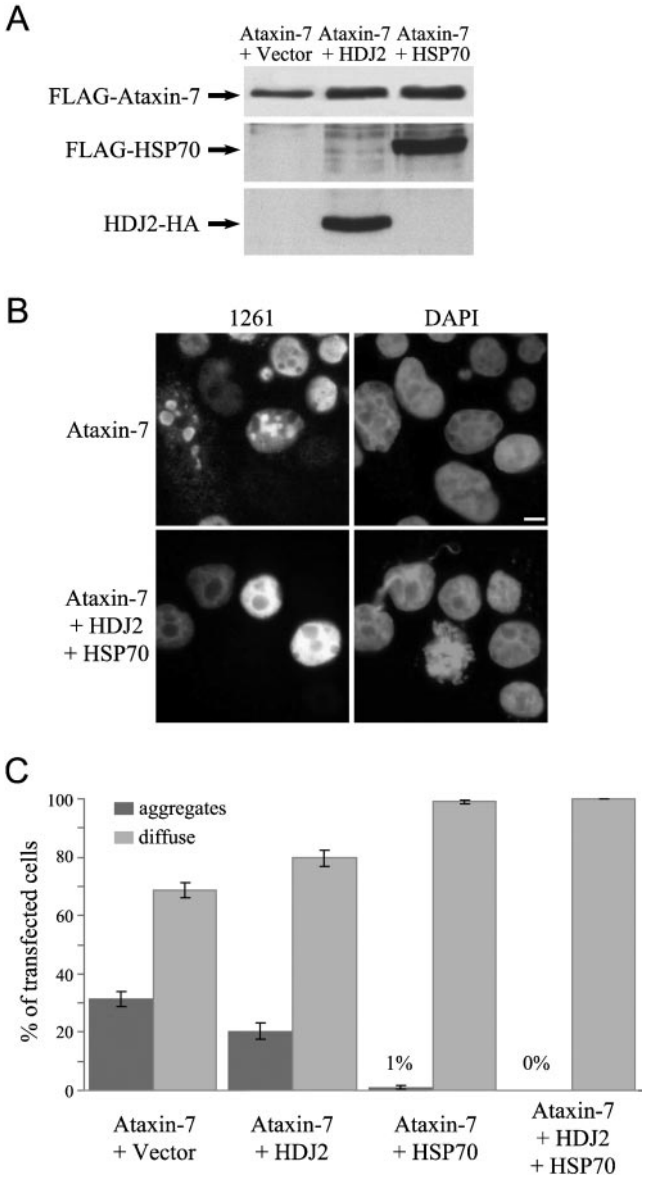

FIG. 1. **HSP70 and HSP40/HDJ2 chaperones can prevent mutant ataxin-7 aggregation in transfected cells.** *A*, HEK293T cells were co-transfected with a full-length mutant *SCA7* cDNA construct (pc7E2FL) and either an empty vector, a human *HDJ2* HA-tagged cDNA construct (pcHDJ2), or a human *HSP70* FLAG-tagged cDNA construct (pcHSP70). Whole cell extracts were prepared 40 h after transfection and analyzed by immunoblotting using an anti-FLAG antibody (*upper* and *middle panels*) or an anti-HA antibody (*lower panel*). *B*, HEK293T cells were co-transfected with pc7E2FL and with either an empty vector or both pcHDJ2 and pcHSP70 constructs (ratio pc7E2FL: pcHDJ2:pcHSP70 1:1:2). Immunolocalization of transiently expressed mutant ataxin-7 (128 Gln) using an anti-ataxin-7 antibody (1261, *left panels*) was performed 24 h after transfection and showed that a significant proportion of transfected cells had nuclear inclusions. When both HDJ2 and HSP70 chaperones were overexpressed, mutant ataxin-7 resulted in homogenous nuclear staining, whereas almost no aggregates could be detected. Nuclei were counterstained with DAPI (*right panels*). The *scale bar* represents 5 μm in each panel. *C*, HEK293T cells were co-transfected with a truncated mutant *SCA7* cDNA construct (pc7E2–456) and either with an empty vector or pcHDJ2, pcHSP70, or both constructs. Immunolocalization of ataxin-7 was performed 24 h after transfection and the percentage of transfected cells with nuclear inclusions (*dark gray bars*) or displaying diffuse nuclear staining (*light gray bars*) was counted in each condition. Each *bar* represents the mean ± S.E. of at least three independent experiments.

results show that mutant ataxin-7 aggregation can be suppressed in transfected cells by manipulating HSP70 and HDJ2 chaperone expression levels.

Generation of Transgenic Lines Overexpressing HDJ2 or HSP70 in the Retina—We then wanted to address whether HSP70 and/or HDJ2 overexpression could modulate mutant ataxin-7 aggregation and neuronal toxicity in a SCA7 mouse model. We previously generated SCA7 transgenic mice (R7E) that highly and specifically overexpress mutant ataxin-7 (90Q) in a single cell type, rod photoreceptors. These mice (from the R7E.A line) have an early and severe retinal dysfunction, as revealed by a progressive decrease of rod photoreceptor electrophysiological activity (9, 29).

We thus made new transgenic mice that co-express molecular chaperones and mutant ataxin-7 in the same cells, at comparable levels and with the same time course. We constructed expression vectors with human *HSP70* or *HDJ2* cDNAs downstream from the same 2.2 kb of the human rhodopsin promoter used to drive mutant ataxin-7 expression. To assess recombinant chaperone expression, we FLAG-tagged *HSP70* and HA-tagged *HDJ2* cDNAs (Fig. 2*A*). The FLAG tag was inserted at the N-terminal end of HSP70 to preserve the integrity of its C-terminal co-chaperone binding domain, while the HA tag was inserted at the C-terminal end of HDJ2 to avoid interference with the structure of its N-terminal J domain (30, 31). We generated several transgenic lines containing *HSP70* or *HDJ2* transgenes and called RH70 and RH40, respectively. They express the recombinant chaperones at different levels relative to the endogenous proteins (Fig. 2*B* and Table I), as determined by Western blot analysis of retinal homogenates using anti-HSP70 or anti-HDJ2 antibodies. RH40 line B and RH70 line G showed the highest expression, reaching 5–10-fold the endogenous levels. Expression levels of endogenous Hsp70 and Hdj2 were not modified in transgenic mice compared with wild type (Fig. 2*B*). Immunostaining with either anti-tag or anti-chaperone antibodies indicated that expression was high and clearly restricted to rod photoreceptors (Fig. 2*C*). In RH40 line E and RH70 line H, we observed strong expression of recombinant chaperones confined to a small subset of rods, accounting for moderate levels detected by Western blots. Finally, chaperone overexpression did not affect retinal structure and function, as revealed by histological examination and electroretinogram recordings (Fig. 2*C* and data not shown).

HSP70/HDJ2 Overexpression, Alone or in Combination, Does Not Modulate SCA7 Retinopathy—F2 hemizygous animals from RH70 line G and RH40 line B were cross-bred with hemizygous R7E mice to generate double transgenic mice R7E/RH70 and R7E/RH40, respectively. This breeding scheme results in all genotypes (wild-type, R7E, RH70, RH40, and double transgenic mice) from the same litter. Rod photoreceptor function was quantified on living animals at 9 weeks of age by measuring the amplitude of the a-wave from electroretinogram recordings performed on dark-adapted mice (scotopic ERGs). At this age, RH70 and RH40 mice displayed similar ERG recordings to that of wild-type littermates (data not shown). We previously showed that rod activity was reduced by around 65% in 9-week-old R7E mice compared with wild-type littermates. These results were obtained with mice maintained on a pure C57BL/6 genetic background (29). As our breeding scheme generated mice with a mixed background (87.5% C57BL/6, 12.5% FVB/N, see "Experimental Procedures"), we first performed ERG recordings on R7E and control mice from these litters. Rod response was only reduced by 40% in 9-week-old R7E mice as compared with control (*CT*) littermates, indicating a slightly less severe disease progression on this mixed background (Fig. 3).

A comparable reduction of rod response was observed between age-matched R7E (106 ± 11 μV), R7E/RH40 (120 ± 16 μV), and R7E/RH70 (94 ± 14 μV) mice as compared with

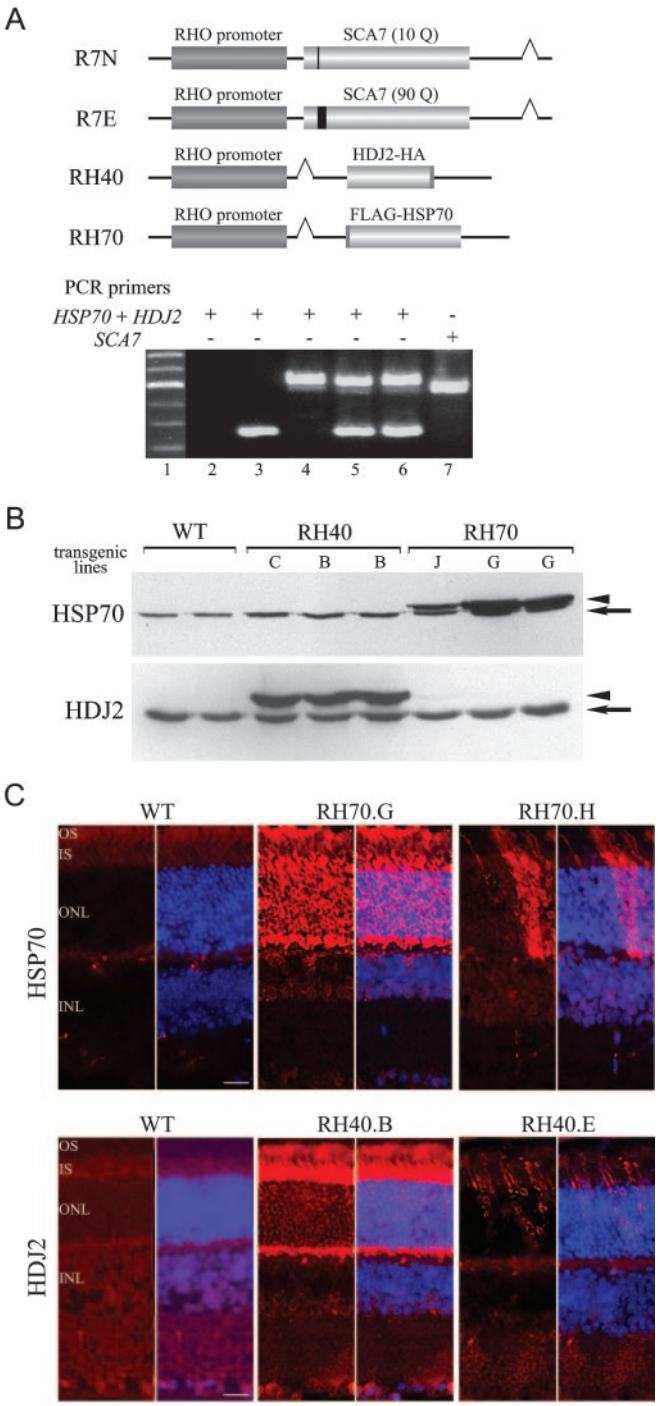

FIG. 2. **Expression of recombinant HSP70 and HDJ2 in transgenic mouse retina.** *A*, schematic view of the transgene constructs generated and used in this study. A representative PCR genotyping of the different transgenic mice is shown below and demonstrates unambiguous determination of all genotypes analyzed in this study (*lane 2*, wild type; *lane 3*, RH40; *lane 4*, RH70; *lane 5*, RH40/RH70 double transgenic; *lanes 6* and *7*, R7E/RH40/RH70 triple transgenic animal; *lane 1*, 100-bp DNA ladder). *B*, analysis of protein expression in 1-month-old WT, RH40 (*lines C* and *B*), and RH70 (*lines J* and *G*) transgenic mice. Western blots of retinal homogenates were probed with anti-HSP70 or anti-HDJ2 antibodies. Recombinant tagged HSP70 or HDJ2 (*arrowheads*) were detected above endogenous Hsp70 or Hdj2 (*arrows*) allowing to estimate recombinant proteins expression levels relative to endogenous chaperones levels. *C*, immunofluorescence of retina from 1-month-old WT, RH40 (*lines B* and *E*), and RH70 (*lines G* and *H*) transgenic animals using anti-HSP70 or anti-HDJ2 antibodies. Faint staining was detected in wild-type retina (*left panels*). In contrast, strong HSP70 and HDJ2 immunoreactivities were found exclusively in photoreceptors of RH70.G and RH40.B retina (*middle panels*). Finally, strong HSP70 and HDJ2 staining were observed in a very restricted number of photoreceptors in RH70.H and RH40.E retina (*right panels*). Both recombinant and endogenous HSP70 and HDJ2 were found in the photoreceptors cytoplasm, particularly within the outer and the inner segments, respectively. Each panel is divided in two showing HDJ2/HSP70 immunoreactivities (*left*) or merged image after counterstaining with DAPI (*right*). *OS*, outer segment; *IS*, inner segment; *ONL*, outer nuclear layer; *INL*, inner nuclear layer. The *scale bar* represents 20 μm in each panel.

TABLE I
Summary of the different HSP70/HDJ2 transgenic mouse lines generated

Construct	No. founders	Lines[a]	Protein expression[b]
RH40	12	A	++[c]
		B	+++
		C	+++
		D	+
		E	+
		F	++
RH70	16	G	+++
		H	+
		I	++
		J	++

[a] Only lines that stably transmitted the transgene over three generations and expressed detectable levels of protein are presented.
[b] Estimated by Western blot analysis using anti-HDJ2 and anti-HA antibodies or anti-HSP70 and anti-FLAG antibodies.
[c] Recombinant/endogenous chaperones expression ratio: +++, >5-fold; ++, around 1-fold; +, <1-fold.

control littermates (182 ± 13 μV) (Fig. 3*B*). As it has been previously shown that HSP70 and HDJ2 act synergistically in preventing polyQ-induced toxicity (25), we then generated triple transgenic mice to overexpress both HSP70 and its co-factor HDJ2 in rod photoreceptors of R7E mice. At 9 weeks of age, ERG recordings showed that rod photoreceptor responses were comparable in R7E/RH40/RH70 (107 ± 11 μV) and R7E (106 ± 11 μV) mice (Fig. 3).

We previously reported that progressive reduction of rod photoreceptor activity was accompanied by dramatic thinning of the segment layer in R7E mice. We assessed progression of retinopathy by histological examination of retina from the 10-week-old R7E, R7E/RH40/RH70 triple transgenic, and WT mice that had been used for the ERG recordings. Toluidin blue-stained retinal sections from triple transgenic R7E/RH40/RH70 or R7E mice were indistinguishable (Fig. 4*A*). At this age, mice of both genotypes displayed heterogeneous pattern of segment loss, accounting for the wavy shape adopted by the photoreceptor nuclear layer (*ONL*). Massive loss of the outer segments is likely due to a failure of rods to renew their segments. Indeed, we previously reported an early down-regulation of rhodopsin expression in R7E mice (29). We thus quantified *Rho* mRNA levels by performing quantitative RT-PCR on RNA extracted from R7E, R7E/RH40/RH70 triple transgenic, and WT retina. At 10 weeks of age, *Rho* mRNA levels were reduced to 9% ± 2% in retinal extracts from R7E mice compared with wild-type mice. A similar down-regulation of *Rho* expression was observed in retina from R7E/RH40/RH70 mice (10% ± 4%) (Fig. 4*B*). Taken together, these results indicate that high and specific overexpression of either HSP70, HDJ2, or both molecular chaperones does not overcome rod photoreceptor dysfunction and is not sufficient to counteract poly(Q)-induced toxicity in this SCA7 model.

We previously showed that the mutant *SCA7* transgene in R7E mice, which is controlled by the rhodopsin promoter, is transiently expressed with less than 5% residual expression from 6 weeks of age (29). We wondered whether recombinant chaperone expression would be affected in R7E/RH40 or in R7E/RH70 mice. Western blot analysis of retinal extracts showed a 2-fold reduction of recombinant HDJ2 levels in 10-

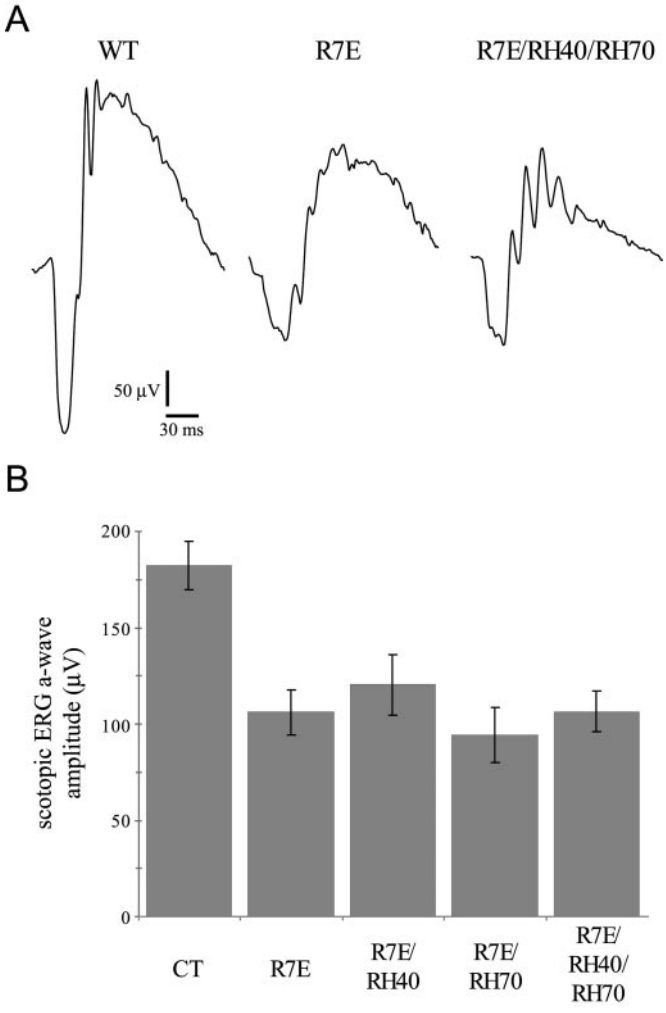

FIG. 3. **Overexpression of HSP70 and HDJ2 does not modulate rod photoreceptors dysfunction in SCA7 mice.** *A*, scotopic ERG responses of WT, R7E, and R7E/RH40/RH70 triple transgenic mice at 9 weeks of age. Each recording corresponds to the average response of one animal at maximal light intensities (from 0 to 1.4 log candela s m^{-2}). Single recordings revealed a similar decrease of rod electrophysiological activity in R7E and R7E/RH40/RH70 mice. *B*, scotopic ERG responses from R7E, R7E/RH40, R7E/RH70, R7E/RH40/RH70 transgenic mice and control littermates (*CT*) at 9 weeks of age ($n = 6$–12 for each group). Rod photoreceptors activity is quantified as the mean amplitude of the a-wave recorded at the four maximal light stimulus intensities (from 0 to 1.4 log candela s m^{-2}). Quantification of rod dysfunction revealed a similar decline in electrophysiological activity in all the genotypes studied compared with control mice. Each bar represents the mean value ± S.E. of 6–12 animals in each group.

week-old R7E/RH40 double transgenic mice, compared with RH40 littermates (Fig. 4*C*). Recombinant HDJ2 levels were still higher than endogenous Hdj2 in R7E/RH40 mice (Fig. 4*C*). Similar observations were made for recombinant HSP70 levels, as a FLAG antibody detected a significant signal in R7E/RH40/RH70 mice (Fig. 5*D*). Thus, the decrease of recombinant chaperone expression was less severe than *SCA7* transgene repression in R7E mice, indicating that the absence of a protective effect is unlikely to be due to HSP70/HDJ2 down-regulation.

HSP70/HDJ2 Overexpression Has No Effect on Mutant Ataxin-7 Aggregation in Vivo—Despite the lack of functional improvement in R7E/RH40/RH70 triple transgenic mice, we examined whether mutant ataxin-7 aggregation is modulated by overexpression of these molecular chaperones. We performed immunostaining using an anti-ataxin-7 antibody to detect NIs in retinal cryosections from 10-week-old R7E and R7E/RH40/RH70 triple transgenic mice. In marked contrast with what was observed in transfected cells, NI content was indistinguishable between R7E (Fig. 5, *A* and *B*) and R7E/RH40/RH70 (Fig. 5, *C* and *D*) retina. At this age, all ataxin-7 immunoreactivity is concentrated into a single, intense nuclear aggregate in most rod nuclei. These NIs were distributed throughout the whole photoreceptor nuclear layer and were of similar size in R7E and R7E/RH40/RH70 retina. Immunostaining using anti-HA or anti-FLAG antibodies indicated that recombinant HDJ2 or HSP70 were not recruited into NIs (Fig. 5, *C* and *D*). These findings indicate that overexpression of HSP70 together with its co-factor HDJ2 is not sufficient to prevent aggregate formation in this SCA7 mouse model. The differential effect of molecular chaperones on mutant ataxin-7 aggregation between cellular and mouse models suggest that the aggregation process is different *in vitro* and *in vivo*.

Proteolytic Processing and Aggregate Formation of Mutant Ataxin-7—As NI formation in R7E mice is not suppressed by HSP70/HDJ2 overexpression, we addressed what might differentiate mutant ataxin-7 aggregation in transfected cells *versus* transgenic mice. Yvert *et al.* (9) previously reported that NIs are composed of an N-terminal fragment of mutant ataxin-7 in R7E mice. Proteolytic processing of mutant ataxin-7 was confirmed in another transgenic SCA7 model and in the brain of a SCA7 patient (14, 32). We thus examined whether mutant ataxin-7 is cleaved in transfected HEK293T cells. We performed immunostaining using anti-ataxin-7 antibodies that recognize either N-terminal (2A10) or C-terminal (1598) epitopes 48 h after transfecting vector that express full-length mutant *SCA7* cDNA carrying 128 CAGs. Both antibodies stained mutant ataxin-7, whether it displayed homogenous nuclear staining or was aggregated into multiple NIs (Fig. 6*B*). This result indicates that, in transfected cells, NIs are formed by full-length mutant ataxin-7. Similarly, aggregation of full-length ataxin-7 in NIs was independently reported by Zander *et al.* (14). We next assessed whether mutant ataxin-7 proteolytic processing occurred in R7E/RH40/RH70 triple transgenic mice. To confirm and better characterize this proteolytic event, we generated a new polyclonal antibody (1599) raised against a synthetic peptide corresponding to amino acids 226–245 of human ataxin-7. Western blots of retinal homogenates from R7N mice (R7N.C line), which overexpress normal ataxin-7 (10Q) in rod photoreceptors, were probed with the purified 1599 antibody. Full-length recombinant ataxin-7 was detected in whole cell extracts from both R7N retina and cells transfected with *SCA7* cDNA constructs (Fig. 6*D*). The 1599 antibody also detected a cross-reacting band in both WT and R7N animals. However, immunostaining of retina cryosections showed that this antibody specifically detected recombinant ataxin-7 in rod photoreceptor nuclei in R7N (Fig. 6*C*) but not in WT mice (data not shown), similarly to what was observed using other specific anti-ataxin-7 antibodies (Fig. 6*C*, *upper panels*). In both R7E and R7E/RH40/RH70 mice, an N-terminal antibody (1261) stained NIs in most rod photoreceptors, while the two more C-terminal antibodies (1599 and 1598), recognizing different epitopes, failed to detect NIs (Fig. 6*C*, *middle* and *lower panels*). These results indicate that NIs are composed of an N-terminal fragment of mutant ataxin-7 and that this processing is not affected by HSP70/HDJ2 overexpression. In transfected cells, the aggregation process is markedly different, as indicated by the fact that NIs are composed of the full-length mutant protein and that chaperone overexpression could suppress full-length or truncated mutant ataxin-7 aggregation. These discrepancies suggest that mutant ataxin-7 processing is markedly different *in vitro* from the *in vivo* situation and might provide one explanation for why chaperone overexpression has

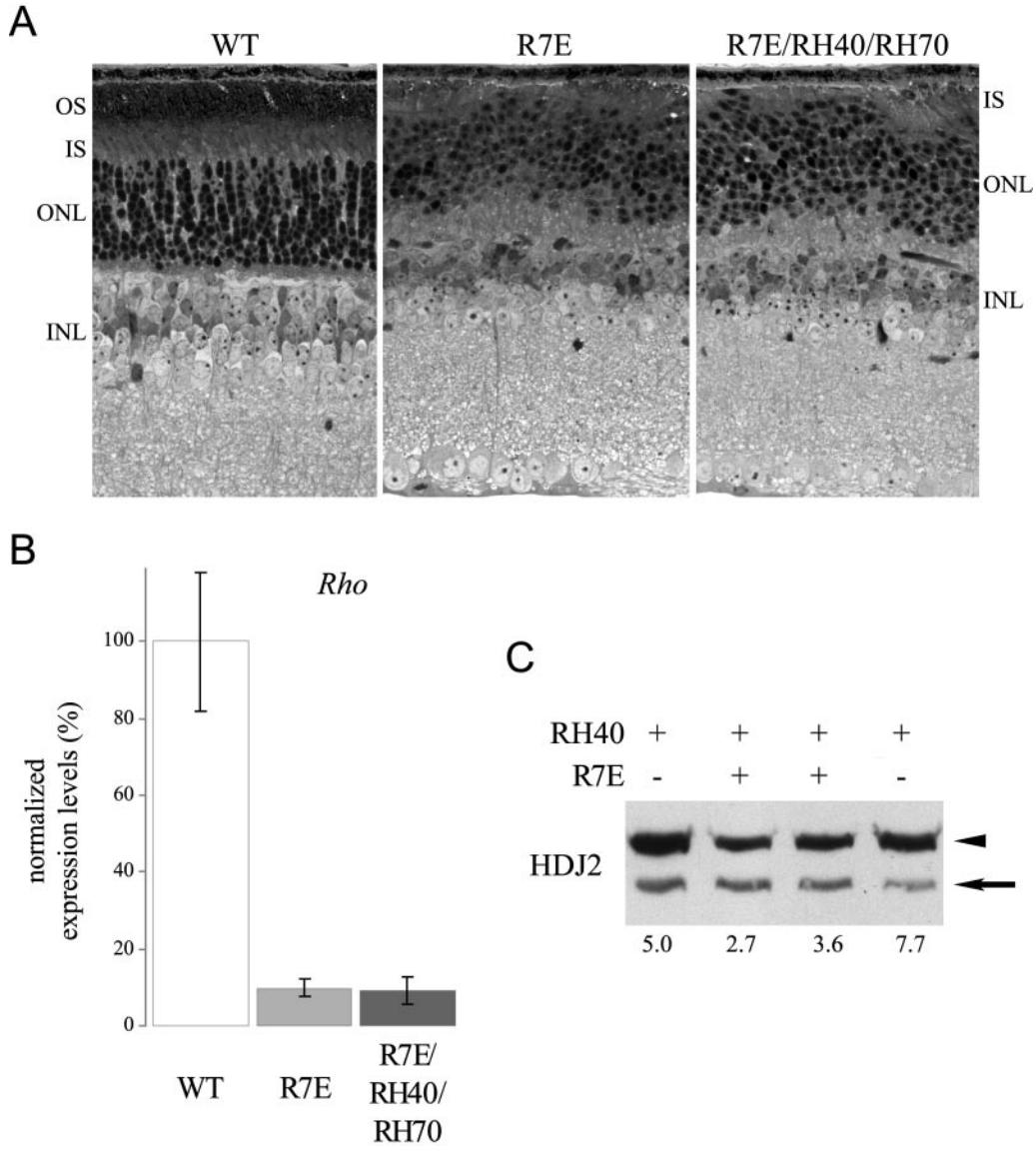

FIG. 4. **Absence of rescue at the histological and molecular levels.** *A*, histological examination of WT, R7E, and R7E/RH40/RH70 triple transgenic mice at 10 weeks of age. Semi-thin toluidin blue-stained sections revealed that the photoreceptor nuclear layer (*ONL*) is disrupted. There are numerous "waves" that correspond to focal loss of the outer segments (*OS*) and thinning of the inner segements (*IS*) in both R7E and R7E/RH40/RH70 mice. *OS*, outer segment; *IS*, inner segment; *ONL*, outer nuclear layer; *INL*, inner nuclear layer. *B*, rhodopsin mRNA levels are severely reduced in both R7E and R7E/RH40/RH70 mice. Quantification of *Rho* expression in control, R7E, and R7E/RH40/RH70 mice at 10 weeks of age ($n = 4$ for each group) by real-time RT-PCR using primers specific for *Rho* and *Ppia* as an internal control. Down-regulation of *Rho* mRNA is comparable in R7E and R7E/RH40/RH70 mice. *Rho* levels are represented as a percentage of the mean of control (*CT*) littermate mice, after normalization to *Ppia* levels. Each *bar* represents the mean value ± S.E. *C*, analysis of recombinant HDJ2 expression in 10-week-old RH40 and R7E/RH40 mice. The Western blot of retinal homogenates was probed with an anti-HDJ2 antibody and quantified by densitometric analysis. Recombinant HDJ2 (*arrowhead*) was normalized to endogenous Hdj2 (*arrow*) levels. Ratios are indicated at the *bottom* of the gel for each mouse. There is a 2-fold reduction of recombinant HDJ2 levels in the R7E background at this age.

no beneficial effects on aggregate formation and eventually on neuronal dysfunction in this SCA7 model.

DISCUSSION

This report demonstrates that high level expression of HSP70 together with its co-factor HDJ2 does not afford protection against poly(Q)-induced toxicity in a mouse model of a poly(Q) disease. The retinopathy in our SCA7 mouse model offers an excellent opportunity to reproducibly quantify the progressive dysfunction of a single cell type and thus to assess the protective effects of chaperone overexpression in mice. We thus generated transgenic lines expressing HSP70 and/or HDJ2 at high levels specifically in rod photoreceptors and backcrossed them with R7E mice. Rod dysfunction was not overcome in R7E mice overexpressing both HSP70 and HDJ2, as assessed by the similar reduction of ERG responses and the comparable histological and transcriptional abnormalities.

Several control experiments were performed to check that the absence of rescue was not due to flaws in our experimental design. First, we controlled that our tagged *HSP70/HDJ2* transgenes retained a refolding activity. These constructs were indeed able to interfere with mutant ataxin-7 aggregation, as shown by the complete inhibition of NI formation after overexpressing FLAG-tagged HSP70 and HA-tagged HDJ2 in transfected HEK293T cells (Fig. 1). Furthermore, this observation indicates that mutant ataxin-7 misfolding and aggregation can be prevented by molecular chaperones in cells, as observed for other polyQ-containing proteins (7, 33–43). Then, we confirmed that rod photoreceptors can simultaneously express multiple transgenes controlled by the same promoter by generating

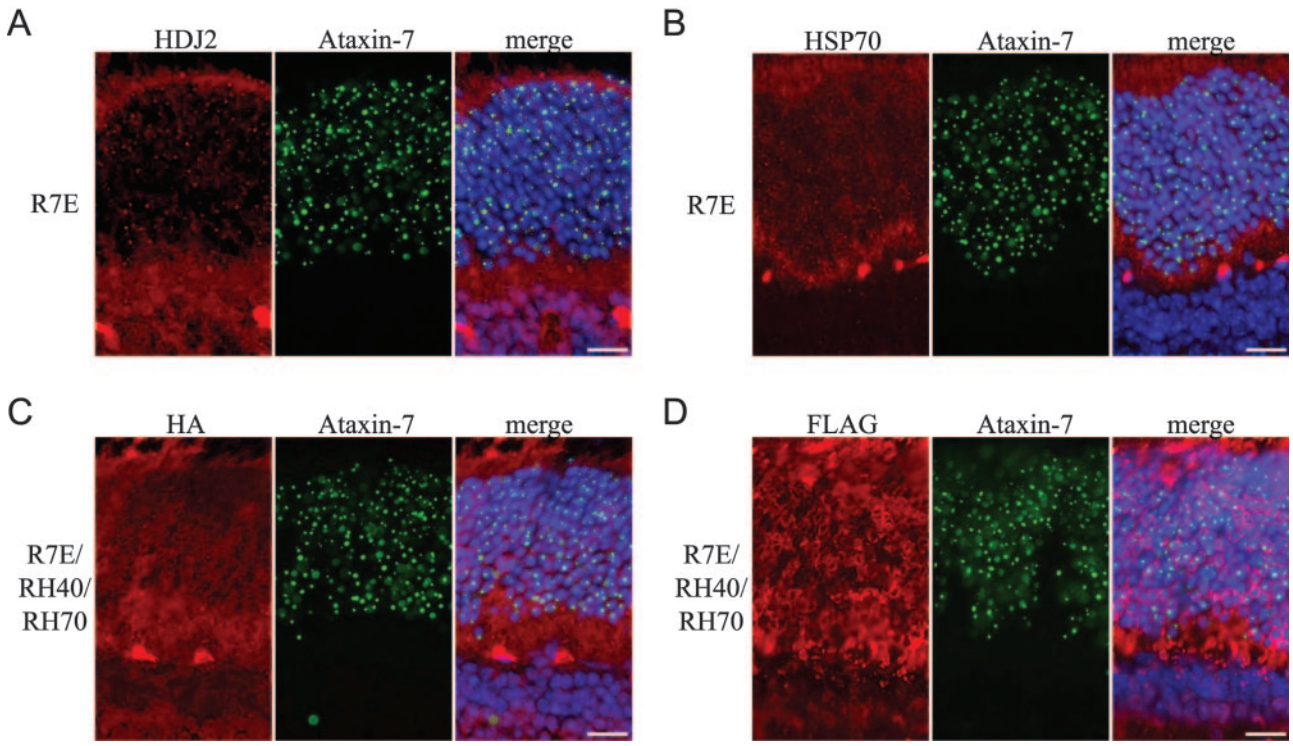

FIG. 5. **Hsp70 and Hdj2 do not suppress aggregates formation in SCA7 mice.** Retinal cryosections (10 μm) from R7E (*A* and *B*) and R7E/RH40/RH70 triple transgenic mice (*C* and *D*) at 10 weeks of age were immunostained using anti-ataxin-7 (*1261*), anti-HDJ2 (*A*), anti-HSP70 (*B*), anti-HA (*C*), and anti-FLAG (*D*) antibodies. Numerous mutant ataxin-7 nuclear aggregates (*green*) were found throughout the photoreceptor nuclear layer from both genotypes (compare *A* and *B* with *C* and *D*). Endogenous Hdj2 was recruited into nuclear inclusions (*red*, *A*). Recombinant HDJ2 and HSP70, detected using anti-tag antibodies, did not co-localize with mutant ataxin-7 (red, panels *C* and *D*). Nuclei were counterstained with DAPI. The *scale bar* represents 10 μm.

double transgenic RH70/RH40 or R7N/RH40 mice. In both cases, the expression levels of both recombinant proteins were similar to those observed in single transgenic mice (data not shown). Furthermore, homozygous RH40 and RH70 mice showed 2-fold higher mRNA and protein levels as compared with hemizygotes (data not shown). This suggests that rods from triple transgenic mice can overexpress different transgenes at the expected levels. Finally, Muchowski *et al.* (44) showed that HSP70, in conjunction with HSP40, efficiently inhibited poly(Q) aggregation only when added during the early phase of the process but failed to inhibit polymerization once seeding has occurred. In this study, the respective transgenes were all controlled by the same promoter, leading to an identical onset of expression, in the same cell type and at comparable levels. We previously reported that poly(Q) expansions repress rhodopsin promoter activity, resulting in repression of *SCA7* transgene expression (29). Similarly, *HDJ2* and *HSP70* transgene expression was also affected but to a lesser extent than the *SCA7* transgene. Thus, in R7E/RH40/RH70 triple transgenics, rod photoreceptors expressed recombinant ataxin-7, HSP70, and HDJ2 at comparable levels during the time course of SCA7 retinopathy.

Polyglutamine aggregates are highly dynamic structures that sequester various proteins either irreversibly or transiently (45–47). In R7E mice, NIs are also dynamic rather than permanent structures, as we previously reported partial clearance of aggregates after loss of mutant *SCA7* transgene expression (29). Expression of both HSP70 and HDJ2 in R7E mice had no effect on the number and size of nuclear inclusions (Fig. 5), indicating that mutant ataxin-7 aggregation was not altered. This observation may not be sufficient to explain why overexpressed chaperones have no beneficial effect on SCA7 retinopathy. While it is clear that progressive accumulation of poly(Q)-containing proteins is a key pathogenic event, the exact role of aggregation in neurodegeneration is not fully understood (6, 48). NI formation could be dissociated from neuronal toxicity in one SCA1 mouse model (49, 50). Furthermore, chaperone modulation of poly(Q) neurodegeneration in flies and of SCA1 motor impairment in mice was not accompanied by a reduction in aggregate formation (19, 21, 27). Although mature aggregates are the observable outcome of the aggregation process, poly(Q) toxicity might stem from earlier oligomer intermediates, which are difficult to detect and quantify (51–53). Interestingly, some studies have suggested that chaperone overexpression renders poly(Q) aggregates more sensitive to detergent solubilization (17, 25). In R7E mice, HSP70/HSP40 chaperone overexpression had no effect on the SDS-extractability of mutant ataxin-7 aggregates (data not shown). In marked contrast, the same molecular chaperones completely suppressed mutant ataxin-7 aggregation in transfected cells, similarly to numerous previous studies.

Many nonexclusive explanations may account for the differential effects of molecular chaperones on poly(Q) aggregation in cellular and animal models. In transfected cells, NIs become visible by light microscopy as early as 1 day after overexpression of poly(Q) proteins, whereas in most transgenic mouse models, aggregates are detectable a few weeks after the onset of expression (9, 50, 54). In cell-based models, the massive and rapid overload of poly(Q) proteins might hide specific or unspecific molecular events associated with continuous formation and processing of aggregates *in vivo*. We observed that mutant ataxin-7 is proteolytically processed in transgenic mice but not in transfected cells. This discrepancy suggests that the full-length protein is handled differently *in vivo*. However, we could not assess whether mutant ataxin-7 is specifically cleaved or non-specifically trimmed, since the aggregated protein could not be resolubilized using standard procedures. Furthermore, HSP70/HSP40 chaperones were able to handle aggregates

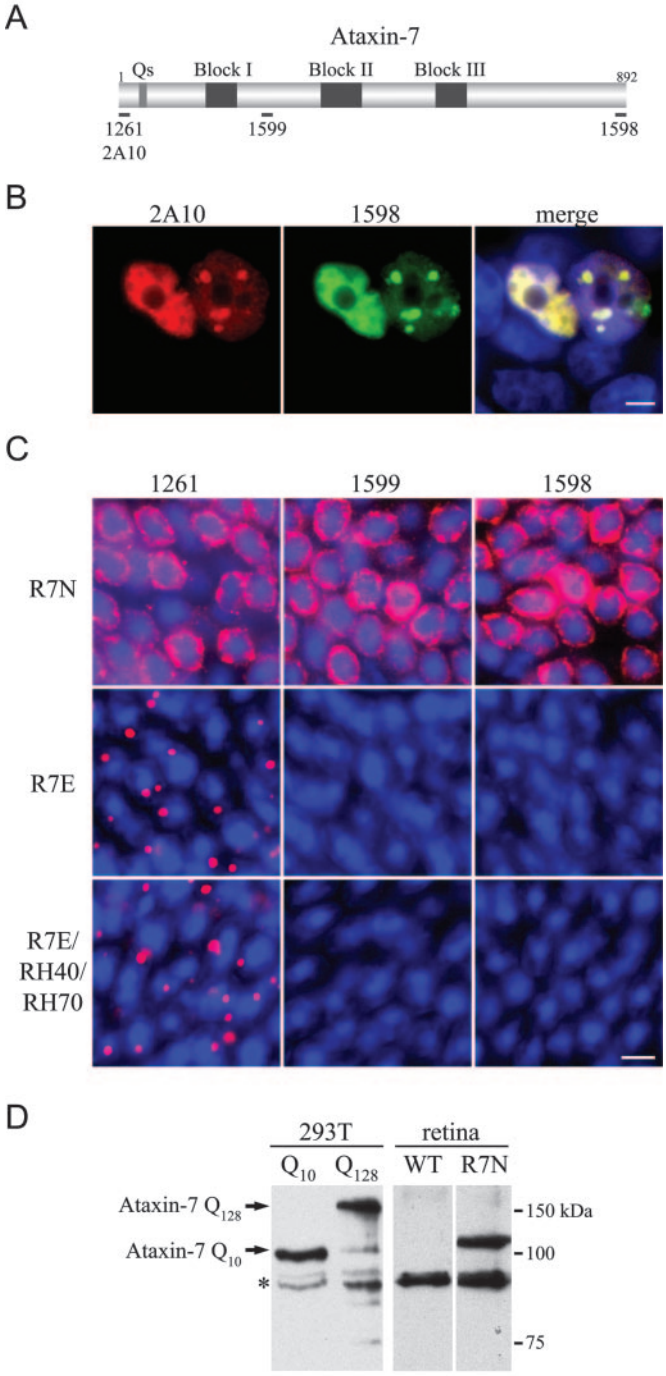

FIG. 6. **Nuclear inclusions contain different forms of ataxin-7 in transfected cells and SCA7 mice.** *A*, schematic representation of human ataxin-7 indicating the positions of the epitopes recognized by the antibodies used in this study. *B*, HEK293T cells were transfected with a full-length mutant *SCA7* cDNA construct (pc7E2FL). Immunolocalization of transiently expressed mutant ataxin-7 (128 Gln), using an N-terminal monoclonal antibody (2A10, *red*) and a C-terminal polyclonal antibody (1598, *green*) was performed 24 h after transfection. The merged image shows that nuclear inclusions are labeled by both antibodies, indicating that NIs are composed of full-length mutant ataxin-7. *C*, retinal cryosections (10 μm) from R7N, R7E, and R7E/RH40/RH70 mice at 10 weeks of age were immunostained using anti-ataxin-7 antibodies (1261, 1599, and 1598) covering the full-length protein. Normal ataxin-7 was stained with all antibodies (*upper panels*) and displayed a characteristic nuclear staining in rod photoreceptors. In contrast, mutant ataxin-7 accumulated in NIs that were detected using N-terminal antibodies (1261) but not using more C-terminal antibodies (1599 and 1598) in R7E mice (*middle panels*). Similar results were obtained in R7E/RH40/RH70 mice (*lower panels*) indicating that C-terminal sequences are lost in both genotypes. Nuclei were counterstained with DAPI. The *scale bar* represents 5 μm. *D*, 1599 polyclonal antibody recognizes normal and mutant ataxin-7 by Western blot. Whole cell extracts of HEK293T cells transfected with full-length normal (pc7NFL) or mutant (pc7E2FL) *SCA7* cDNA constructs were analyzed by Western blot using 1599 antibody. Bands corresponding to normal (10 Gln) and mutant (128 Gln) ataxin-7 were specifically revealed by 1599 at the expected sizes (110 and 160 kDa, respectively). Western blot of retinal homogenates from WT or R7N mice confirmed that 1599 recognizes normal recombinant ataxin-7 at the expected size (110 kDa). A nonspecific cross-reacting band of lower molecular weight (*asterisk*) was detected in both WT and R7N retina.

formed in cells transfected with constructs encoding full-length or truncated mutant ataxin-7 (Fig. 1*C*). Thus, proteolytic processing of ataxin-7 in transgenic mice might be one out of a number of nonexclusive molecular mechanisms, which altogether account for the differential sensitivity of poly(Q) aggregates to molecular chaperones in different model systems.

So far, the protective effects of chaperones have been investigated by crossing SCA1, SBMA, and HD transgenic models with mice that overexpress HSP70 ubiquitously. HSP70 overexpression in SBMA mice improved their motor phenotype and survival rate, probably by reducing nuclear translocation of the mutant androgen receptor (55). Similar experiments in SCA1 mice led to a milder amelioration of the motor dysfunction (27), while in R6/2 mice, two independent studies reported no effect on disease progression and survival (17, 28). We show here that even high and specific overexpression of both HSP70 and its co-factor HSP40/HDJ2 did not ameliorate the SCA7 mouse phenotype. Altogether, these observations indicate that chaperone overexpression in mammals might have different effects, depending on the specific features of each poly(Q) protein. In addition, there is a striking discrepancy between these findings and the identification of molecular chaperones as powerful suppressors of poly(Q) toxicity in all fly models generated so far. HSP70 overexpression has been shown to protect flies against other pathological conditions, including α-synuclein toxicity, fragile X premutation, and normal aging (56–58). Molecular chaperones might have beneficial effects by preventing misfolded proteins from adopting toxic conformations or through a variety of other pathways which could be differentially regulated and implicated between model systems. For instance, chaperones might inhibit apoptosis that is triggered by misfolded proteins. Indeed, HSP70 has been shown to counteract the activity of the stress-induced kinase JNK and to negatively regulate the apoptosome (59). At variance with mammalian models, poly(Q) flies are characterized by massive neuronal loss. This phenotype can be fully rescued by overexpression of chaperones, which could exert their beneficial effect via anti-apoptotic functions. Furthermore, the HSP70/HSP40 system helps ubiquitin ligases to recognize and target misfolded proteins for proteasomal degradation (60). Many mechanisms at the crossroads of protein misfolding, protein degradation, and apoptosis could be influenced by chaperones and could contribute to the differential effect of molecular chaperones in invertebrate and mouse models.

In mammals, the high redundancy of the chaperone and ubiquitin-proteasome systems suggest that there are additional protein quality control components which might not be present or required in invertebrates. This redundancy is probably critical for mammals to protect themselves against specific stress associated with an extended neuronal life span or environmental conditions. If many of these additional factors are altered in poly(Q) mouse models, correction of a single pathway would not be sufficient to suppress the neurological phenotype. In agreement with that hypothesis, Hay *et al.* (17) recently reported that there is a decrease in the levels of several heat shock proteins, which correlates with phenotype progression in R6/2 mice, and that pharmacological induction of chaperones

significantly delayed aggregates formation in an organotypic slice culture assay. Thus, induction of a global heat shock response, not exclusively HSP40 and HSP70, might be a more useful therapeutic approach that is worthy of further investigation in mouse models of poly(Q) diseases. Our results also indicate that a better understanding of the molecular mechanisms underlying the discrepancies between cellular, invertebrate, and mouse models would be required before further validation of chaperone induction as a therapeutic strategy.

Acknowledgments—We thank Bohdan Wasylyk for critical reading of the manuscript and K. Merienne for helpful discussion. We thank J. Bennett for gift of the rhodopsin promoter, R. Morimoto for the *HSP70* cDNA, and T. Mohanakumar for the *HDJ2* cDNA and D. Metzger for the pGSp2 plasmid. We are indebted to C. Weber, S. Rousseau, J. Hergueux, and A. Gansmüller for technical assistance and to G. Yvert and G. Duval for 1599 antibody production and to the staff at the Mouse Clinical Institute for microinjections and mouse care.

REFERENCES

1. Michalik, A., Martin, J. J., and Van Broeckhoven, C. (2004) *Eur. J. Hum. Genet.* **12,** 2–15
2. David, G., Abbas, N., Stevanin, G., Durr, A., Yvert, G., Cancel, G., Weber, C., Imbert, G., Saudou, F., Antoniou, E., Drabkin, H., Gemmill, R., Giunti, P., Benomar, A., Wood, N., Ruberg, M., Agid, Y., Mandel, J. L., and Brice, A. (1997) *Nat. Genet.* **17,** 65–70
3. Helmlinger, D., Hardy, S., Sasorith, S., Klein, F., Robert, F., Weber, C., Miguet, L., Potier, N., Van-Dorsselaer, A., Wurtz, J. M., Mandel, J. L., Tora, L., and Devys, D. (2004) *Hum. Mol. Genet.* **13,** 1257–1265
4. Zoghbi, H. Y., and Orr, H. T. (2000) *Annu. Rev. Neurosci.* **23,** 217–247
5. Ross, C. A. (2002) *Neuron* **35,** 819–822
6. Bates, G. (2003) *Lancet* **361,** 1642–1644
7. Cummings, C. J., Mancini, M. A., Antalffy, B., DeFranco, D. B., Orr, H. T., and Zoghbi, H. Y. (1998) *Nat. Genet.* **19,** 148–154
8. Opal, P., and Zoghbi, H. Y. (2002) *Trends Mol. Med.* **8,** 232–236
9. Yvert, G., Lindenberg, K. S., Picaud, S., Landwehrmeyer, G. B., Sahel, J. A., and Mandel, J. L. (2000) *Hum. Mol. Genet.* **9,** 2491–2506
10. Yvert, G., Lindenberg, K. S., Devys, D., Helmlinger, D., Landwehrmeyer, G. B., and Mandel, J. L. (2001) *Hum. Mol. Genet.* **10,** 1679–1692
11. La Spada, A. R., Fu, Y. H., Sopher, B. L., Libby, R. T., Wang, X., Li, L. Y., Einum, D. D., Huang, J., Possin, D. E., Smith, A. C., Martinez, R. A., Koszdin, K. L., Treuting, P. M., Ware, C. B., Hurley, J. B., Ptacek, L. J., and Chen, S. (2001) *Neuron* **31,** 913–927
12. Yoo, S. Y., Pennesi, M. E., Weeber, E. J., Xu, B., Atkinson, R., Chen, S., Armstrong, D. L., Wu, S. M., Sweatt, J. D., and Zoghbi, H. Y. (2003) *Neuron* **37,** 383–401
13. Mauger, C., Del-Favero, J., Ceuterick, C., Lubke, U., van Broeckhoven, C., and Martin, J. (1999) *Brain Res. Mol. Brain Res.* **74,** 35–43
14. Zander, C., Takahashi, J., El Hachimi, K. H., Fujigasaki, H., Albanese, V., Lebre, A. S., Stevanin, G., Duyckaerts, C., and Brice, A. (2001) *Hum. Mol. Genet.* **10,** 2569–2579
15. Takahashi, J., Fujigasaki, H., Zander, C., El Hachimi, K. H., Stevanin, G., Durr, A., Lebre, A. S., Yvert, G., Trottier, Y., The, H., Hauw, J. J., Duyckaerts, C., and Brice, A. (2002) *Brain* **125,** 1534–1543
16. Helmlinger, D., Yvert, G., Picaud, S., Merienne, K., Sahel, J., Mandel, J. L., and Devys, D. (2002) *Hum. Mol. Genet.* **11,** 3351–3359
17. Hay, D. G., Sathasivam, K., Tobaben, S., Stahl, B., Marber, M., Mestril, R., Mahal, A., Smith, D. L., Woodman, B., and Bates, G. P. (2004) *Hum. Mol. Genet.* **13,** 1389–1405
18. Sakahira, H., Breuer, P., Hayer-Hartl, M. K., and Hartl, F. U. (2002) *Proc. Natl. Acad. Sci. U. S. A.* **99.** Suppl. 4, 16412–16418
19. Kazemi-Esfarjani, P., and Benzer, S. (2000) *Science* **287,** 1837–1840
20. Fernandez-Funez, P., Nino-Rosales, M. L., de Gouyon, B., She, W. C., Luchak, J. M., Martinez, P., Turiegano, E., Benito, J., Capovilla, M., Skinner, P. J., McCall, A., Canal, I., Orr, H. T., Zoghbi, H. Y., and Botas, J. (2000) *Nature* **408,** 101–106
21. Warrick, J. M., Chan, H. Y. E., Gray-Board, G. L., Chai, Y., Paulson, H. L., and Bonini, N. M. (1999) *Nat. Genet.* **23,** 425–428
22. Chan, H. Y., Warrick, J. M., Andriola, I., Merry, D., and Bonini, N. M. (2002) *Hum. Mol. Genet.* **11,** 2895–2904
23. Takeyama, K., Ito, S., Yamamoto, A., Tanimoto, H., Furutani, T., Kanuka, H., Miura, M., Tabata, T., and Kato, S. (2002) *Neuron* **35,** 855–864
24. Ghosh, S., and Feany, M. B. (2004) *Hum. Mol. Genet.* **13,** 2011–2018
25. Chan, H. Y., Warrick, J. M., Gray-Board, G. L., Paulson, H. L., and Bonini, N. M. (2000) *Hum. Mol. Genet.* **9,** 2811–2820
26. Hartl, F. U., and Hayer-Hartl, M. (2002) *Science* **295,** 1852–1858
27. Cummings, C. J., Sun, Y., Opal, P., Antalffy, B., Mestril, R., Orr, H. T., Dillmann, W. H., and Zoghbi, H. Y. (2001) *Hum. Mol. Genet.* **10,** 1511–1518
28. Hansson, O., Nylandsted, J., Castilho, R. F., Leist, M., Jaattela, M., and Brundin, P. (2003) *Brain Res.* **970,** 47–57
29. Helmlinger, D., Abou-Sleymane, G., Yvert, G., Rousseau, S., Weber, C., Trottier, Y., Mandel, J. L., and Devys, D. (2004) *J. Neurosci.* **24,** 1881–1887
30. Demand, J., Luders, J., and Hohfeld, J. (1998) *Mol. Cell. Biol.* **18,** 2023–2028
31. Freeman, B. C., Myers, M. P., Schumacher, R., and Morimoto, R. I. (1995) *EMBO J.* **14,** 2281–2292
32. Garden, G. A., Libby, R. T., Fu, Y. H., Kinoshita, Y., Huang, J., Possin, D. E., Smith, A. C., Martinez, R. A., Fine, G. C., Grote, S. K., Ware, C. B., Einum, D. D., Morrison, R. S., Ptacek, L. J., Sopher, B. L., and La Spada, A. R. (2002) *J. Neurosci.* **22,** 4897–4905
33. Chai, Y., Koppenhafer, S. L., Bonini, N. M., and Paulson, H. L. (1999) *J. Neurosci.* **19,** 10338–10347
34. Jana, N. R., Tanaka, M., Wang, G., and Nukina, N. (2000) *Hum. Mol. Genet.* **9,** 2009–2018
35. Mitsui, K., Nakayama, H., Akagi, T., Nekooki, M., Ohtawa, K., Takio, K., Hashikawa, T., and Nukina, N. (2002) *J. Neurosci.* **22,** 9267–9277
36. Ishihara, K., Yamagishi, N., Saito, Y., Adachi, H., Kobayashi, Y., Sobue, G., Ohtsuka, K., and Hatayama, T. (2003) *J. Biol. Chem.* **278,** 25143–25150
37. Stenoien, D. L., Cummings, C. J., Adams, H. P., Mancini, M. G., Patel, K., DeMartino, G. N., Marcelli, M., Weigel, N. L., and Mancini, M. A. (1999) *Hum. Mol. Genet.* **8,** 731–741
38. Kobayashi, Y., Kume, A., Li, M., Doyu, M., Hata, M., Ohtsuka, K., and Sobue, G. (2000) *J. Biol. Chem.* **275,** 8772–8778
39. Sittler, A., Lurz, R., Lueder, G., Priller, J., Lehrach, H., Hayer-Hartl, M. K., Hartl, F. U., and Wanker, E. E. (2001) *Hum. Mol. Genet.* **10,** 1307–1315
40. Zhou, H., Li, S. H., and Li, X. J. (2001) *J. Biol. Chem.* **276,** 48417–48424
41. Bailey, C. K., Andriola, I. F., Kampinga, H. H., and Merry, D. E. (2002) *Hum. Mol. Genet.* **11,** 515–523
42. Chuang, J. Z., Zhou, H., Zhu, M., Li, S. H., Li, X. J., and Sung, C. H. (2002) *J. Biol. Chem.* **277,** 19831–19838
43. Carmichael, J., Chatellier, J., Woolfson, A., Milstein, C., Fersht, A. R., and Rubinsztein, D. C. (2000) *Proc. Natl. Acad. Sci. U. S. A.* **97,** 9701–9705
44. Muchowski, P. J., Schaffar, G., Sittler, A., Wanker, E. E., Hayer-Hartl, M. K., and Hartl, F. U. (2000) *Proc. Natl. Acad. Sci. U. S. A.* **97,** 7841–7846
45. Chai, Y., Shao, J., Miller, V. M., Williams, A., and Paulson, H. L. (2002) *Proc. Natl. Acad. Sci. U. S. A.* **99,** 9310–9315
46. Kim, S., Nollen, E. A., Kitagawa, K., Bindokas, V. P., and Morimoto, R. I. (2002) *Nat. Cell Biol.* **4,** 826–831
47. Stenoien, D. L., Mielke, M., and Mancini, M. A. (2002) *Nat. Cell Biol.* **4,** 806–810
48. Michalik, A., and Van Broeckhoven, C. (2003) *Hum. Mol. Genet.* **12,** R173–R186
49. Klement, I. A., Skinner, P. J., Kaytor, M. D., Yi, H., Hersch, S. M., Clark, H. B., Zoghbi, H. Y., and Orr, H. T. (1998) *Cell* **95,** 41–53
50. Cummings, C. J., Reinstein, E., Sun, Y., Antalffy, B., Jiang, Y., Ciechanover, A., Orr, H. T., Beaudet, A. L., and Zoghbi, H. Y. (1999) *Neuron* **24,** 879–892
51. Yang, W., Dunlap, J. R., Andrews, R. B., and Wetzel, R. (2002) *Hum. Mol. Genet.* **11,** 2905–2917
52. Chen, S., Berthelier, V., Yang, W., and Wetzel, R. (2001) *J. Mol. Biol.* **311,** 173–182
53. Sanchez, I., Mahlke, C., and Yuan, J. (2003) *Nature* **421,** 373–379
54. Davies, S. W., Turmaine, M., Cozens, B. A., Difiglia, M., Sharp, A. H., Ross, C. A., Scherzinger, E., Wanker, E. E., Mangiarini, L., and Bates, G. P. (1997) *Cell* **90,** 537–548
55. Adachi, H., Katsuno, M., Minamiyama, M., Sang, C., Pagoulatos, G., Angelidis, C., Kusakabe, M., Yoshiki, A., Kobayashi, Y., Doyu, M., and Sobue, G. (2003) *J. Neurosci.* **23,** 2203–2211
56. Tatar, M., Khazaeli, A. A., and Curtsinger, J. W. (1997) *Nature* **390,** 30
57. Auluck, P. K., Chan, H. Y., Trojanowski, J. Q., Lee, V. M., and Bonini, N. M. (2002) *Science* **295,** 865–868
58. Jin, P., Zarnescu, D. C., Zhang, F., Pearson, C. E., Lucchesi, J. C., Moses, K., and Warren, S. T. (2003) *Neuron* **39,** 739–747
59. Takayama, S., Reed, J. C., and Homma, S. (2003) *Oncogene* **22,** 9041–9047
60. Berke, S. J., and Paulson, H. L. (2003) *Curr. Opin. Genet. Dev.* **13,** 253–261